To determine the modal gain we have performed gain studies by the variable stripe length method with current injection following the technique described in [6]. In this method the modal gain spectra are extracted from the amplified spontaneous light emitted from the sample edge. The measurements are not limited by the lasing threshold and can be carried out up to high excitation densities. These studies were performed under pulse excitation. The gain spectra are shown in Fig. 4. The maxima at 1.254 and 1.18µm correspond to the ground and first excited state transitions. At current densities of ~900A/cm^2 the gain of the ground state transition saturates. The value of the maximal modal gain of the ground state transition (12cm^{-1}) agrees very well with the result for the broad area devices [2] as well as with the value derived from Fig. 1.

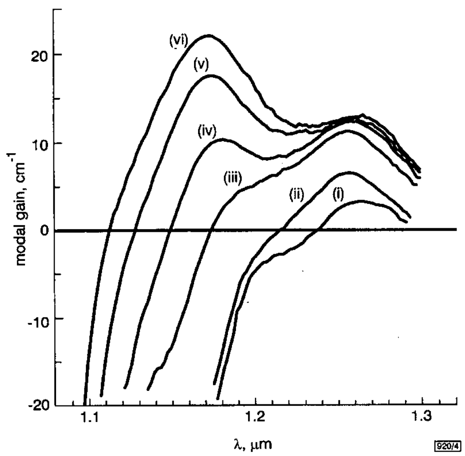

Fig. 4 *Modal gain spectra for different current densities*

(i) 98A/cm^2; (ii) 195A/cm^2; (iii) 487A/cm^2; (iv) 975A/cm^2; (v) 1950A/cm^2; (vi) 2925A/cm^2

Conclusions: We have studied high power single transverse mode long wavelength lasers based on QDs. The maximum output power of these devices is typically ~330mW with singlemode operation observed up to 110mW. The maximal modal gain for the ground state transition measured by using the variable stripe length method is 12cm^{-1}.

Acknowledgments: This work is supported by the Volkswagen Foundation (grant 1/73-631), INTAS (grant 96-0467), BMBF/DRL, NanOp CC, and DAAD and the Program 'Physics of Solid State Nanostructures' of the Ministry of Science of Russia.

14 October 1999

Electronics Letters Online No: 19991392

DOI: 10.1049/el:19991392

M.V. Maximov, Yu. M.Shernyakov, I.N. Kaiander, D.A. Bedarev, E.Yu. Kondrat'eva, P.S. Kop'ev, A.R. Kovsh, N.A. Maleev, S.S. Mikhrin, A.F. Tsatsul'nikov, V.M. Ustinov, B.V. Volovik, A.E. Zhukov and Zh.J. Alferov (*A.F. Ioffe Physical-Technical Institute, Politekhnicheskaya 26, 194021, St. Petersburg, Russia*)

N.N. Ledentsov and D. Bimberg (*Institut für Festkörperphysik, Technische Universität Berlin, Hardenbergstrasse 36, D-10623 Berlin, Germany*)

References

1 HUFFAKER, D.L., PARK, G., ZOU, Z., SHCHEKIN, O.B., and DEPPE, D.G.: '1.3µm room-temperature GaAs-based quantum-dot laser', *Appl. Phys. Lett.*, 1998, **73**, (18), pp. 2564–2566

2 SHERNYAKOV, YU.M., BEDAREV, D.A., KONDRAT'EVA, E.YU., KOP'EV, P.S., KOVSH, A.R., MALEEV, N.A., MAXIMOV, M.V., VOLOVIK, B.V., ZHUKOV, A.E., ALFEROV, ZH.I., LEDENTSOV, N.N., and BIMBERG, D.: '1.3µm GaAs-based laser using quantum dots obtained by activated spinodal decomposition', *Electron. Lett.*, 1999, **35**, (11), pp. 898–900

3 ZHUKOV, A.E., KOVSH, A.R., USTINOV, V.M., SHERNYAKOV, YU.M., MIKHRIN, S.S., MALEEV, N.A., KONDRAT'EVA, E.YU., LIVSHITS, D.A., MAXIMOV, M.V., VOLOVIK, B.V., BEDAREV, D.A., MUSIKHIN, YU.G., LEDENTSOV, N.N., KOP'EV, P.S., ALFEROV, ZH.I., and BIMBERG, D.: 'Continuous wave operation of long-wavelength quantum dot diode laser on a GaAs substrate', to be published in *IEEE Photonics Technol. Lett.*, 1999

4 LIU, G.T., STINTZ, A., LI, H., MALLOY, K.J., and LESTER, L.F.: '1.24µm low threshold current density dots-in-a-well (DWELL) lasers'. IEEE/LEOS Summer Topical Meeting, Workshop on Nanostructures and Quantum Dots, San Diego, CA, USA, 26–27 July 1999, pp. 27–28 (IEEE Catalog Number: 99TH8455)

5 VOLOVIK, B.V., TSATSUL'NIKOV, A.F., BEDAREV, D.A., EGOROV, A.YU., ZHUKOV, A.E., KOVSH, A.R., LEDENTSOV, N.N., MAKSIMOV, M.V., MALEEV, N.A., MUSIKHIN, YU.G., SUVOROVA, A.A., USTINOV, V.M., KOP'EV, P.S., ALFEROV, ZH.I., BIMBERG, D., and WERNER, P.: 'Long-wavelength emission in structures with quantum dots formed in the stimulated decomposition of a solid solution at strained islands', *Semiconductors*, 1999, **33**, (8), pp. 990–995

6 OSTER, A., ERBERT, G., and WENZEL, H.: 'Gain spectra measurement by a variable stripe method with current injection', *Electron. Lett.*, 1997, **33**, (10), pp. 864–866

Polynomial bidirectional hetero-correlator

Chua-Chin Wang and Cheng-Fa Tsai

A novel pattern recognition method is proposed using a polynomial bidirectional hetero-correlator. Simulation results show that the new scheme has a higher storage capacity than other BAM-like associative memories and fuzzy associative memories.

Introduction: The bidirectional associative memory-like (BAM-like) associative memory is a two-layer hetero-associator that stores a set of bipolar pairs. Owing to the ease with which they are encoded and their high noise immunity, BAMs are well-suited to use in pattern recognition, intelligent control and optimisation problems. The original Kosko BAM suffers from low storage capacity [2]. Thus, much effort has been made to improve the performance of the Kosko BAM [1, 3, 5]. In some of these models the BAM architecture is improved by using the Hamming stability learning algorithm (SBAM) [5], the asymmetrical BAM model (ABAM) [3], or by the introduction of a general model of BAM (GBAM) to improve the performance [1]. Kosko's fuzzy associative memory (FAM) is the very first example to use neural networks to articulate fuzzy rules for fuzzy systems. Despite its simplicity and modularity, his model suffers from extremely low memory capacity, i.e. one rule per FAM matrix. Besides, it is limited to small rule-based applications. Chung and Lee [4] proposed a multiple-rule storage method for an FAM matrix. They showed that more than one rule can be encoded by Kosko's FAM. However, the actual capacity will depend on the dimension of the matrix and the rule characteristics, e.g. how many of the rules are overlapped. The capacity of this model depends on whether the membership function is semi-overlapped or not. In this Letter, we present a novel fuzzy data processing method using a polynomial bidirectional hetero-correlator (PBHC). A perfect recall theorem is established and the implementation of the PBHC model is accordingly more efficient. The proposed model has a higher capacity for pattern pair storage than that of conventional BAMs and fuzzy memories.

Proposed polynomial bidirectional hetero-associator: We assume that we are given M pattern pairs, which are $\{(X_1, Y_1), (X_2, Y_2), ..., (X_M, Y_M)\}$, where $X_i = (x_{i1}, x_{i2}, ..., x_{in})$, $Y_i = (y_{i1}, y_{i2}, ..., y_{ip})$. We let $1 \le i \le M$, $x_{ij} \in [0, 1]$, $1 \le j \le n$, $y_{ij} \in [0, 1]$, $1 \le j \le p$, n and p are the component dimensions of X_i and Y_i, and n is assumed to be smaller than or equal to p without any loss of generality. x_{ij}, y_{ij} $\in \{0/\lambda, 1/\lambda, ..., \lambda/\lambda\}$, fuzzy space = [1, 0], λ is a fuzzy quantum, and σ is a fuzzy quantum gap. For instance, by assuming that $\lambda = 10$, $\sigma = 1/\lambda = 0.1$ can be obtained. We use the following evolution equations in the recall process of the PBHC:

$$y_k = H\left(\frac{\sum_{i=1}^{M} y_{ik} \cdot \left((u - \|X_i - X\|^2)/u\right)^{M^Z}}{\sum_{i=1}^{M} \left((u - \|X_i - X\|^2)/u\right)^{M^Z}}\right) \quad (1)$$

$$x_k = H\left(\frac{\sum_{i=1}^{M} x_{ik} \cdot \left((u - \|Y_i - Y\|^2)/u\right)^{M^Z}}{\sum_{i=1}^{M} \left((u - \|Y_i - Y\|^2)/u\right)^{M^Z}}\right) \quad (2)$$

where X_i, Y_i, $i = 1, ..., M$, represent the stored patterns, X or Y is the initial vector presented to the network, x_k and x_{ik} denote the kth digits of X and X_i, respectively, y_k and y_{ik} represent the kth digits of Y and Y_i, respectively, Z is a positive integer, u denotes a function defined by the following equation:

$$u = \sum_{i=1}^{M}\sum_{j=1}^{M} (\|X_i - X_j\|^2 + \|Y_i - Y_j\|^2) \quad (3)$$

and $H(\cdot)$ is a staircase function as shown in the following equation:

$$H(x) = \begin{cases} 0 & x < 1/(2\lambda) \\ \lfloor x + 1/(2\lambda) \rfloor & \text{elsewhere} \end{cases} \quad (4)$$

Note that if $\lambda \to \infty$, then $H(x) \simeq x$, for $x \in [0, 1]$. Also, u is bounded according to eqn. 3.

The signal-to-noise ratio (SNR) approach is adopted here to compute the capacity of the PBHC. We let X_i and Y_i be the stored pattern pairs, and assume that X_1 is the input pattern pair and Y_1 is recalled expectantly. Substituting X_1 for X allows us to rewrite eqn. 1 as (note that if $\lambda \to \infty$, then $H(x) \simeq x$, for $x \in [0, 1]$)

$$\begin{aligned} y_k &= H\left(\frac{\sum_{i=1}^{M} y_{ik} \cdot \left((u - \|X_i - X\|^2)/u\right)^{M^Z}}{\sum_{i=1}^{M} \left((u - \|X_i - X\|^2)/u\right)^{M^Z}}\right) \\ &\simeq \left(\frac{\sum_{i=1}^{M} y_{ik} \cdot \left((u - \|X_i - X\|^2)/u\right)^{M^Z}}{\sum_{i=1}^{M} \left((u - \|X_i - X\|^2)/u\right)^{M^Z}}\right) \\ y_k &\cdot \sum_{i=1}^{M} \left((u - \|X_i - X\|^2)/u\right)^{M^Z} \\ &= \sum_{i=1}^{M} y_{ik} \cdot \left((u - \|X_i - X\|^2)/u\right)^{M^Z} \\ &= y_{1k} \cdot 1^2 + y_{2k} \cdot \left((u - \|X_2 - X_1\|^2)/u\right)^{M^Z} + \cdots \\ &\quad + y_{Mk} \cdot \left((u - \|X_M - X_1\|^2)/u\right)^{M^Z} \quad (5) \end{aligned}$$

The largest noise that can appear is that any X_i, $i \neq 1$, is just one component different from X_1, and the difference in the corresponding component is only $1/(2\lambda)$. Meanwhile, the other components of X_i and X_1 remain the same. For instance, $X_1 = (x_{11}, x_{12}, ..., x_{1n})$, and $X_i = (x_{11}, x_{12}, ..., x_{1n} \pm 1/(2\lambda))$, $i \neq 1$, where $x_{ik}, y_{ik} \in \{0/\lambda, 1/\lambda, ..., \lambda/\lambda\}$. The first term in the previous equation corresponds to the signal, and the other terms are the noise. Besides the first term, the remaining terms are actually the sum of $M - 1$ times the noise of a single noise term, e.g. y_{2k}. From eqn. 5, the following inequalities can be obtained:

$$\begin{aligned} y_k &\le y_k \cdot \sum_{i=1}^{M} \left((u - \|X_i - X\|^2)/u\right)^{M^Z} \\ &\le y_{1k} \cdot 1^2 + \sum_{j=2}^{M} y_{jk} \cdot \left((u - 1/\lambda^2)/u\right)^{M^Z} \\ &\le y_{1k} \cdot 1^2 + (M-1) y_{2k} \cdot \left((u - 1/\lambda^2)/u\right)^{M^Z} \\ &= S + N_{max} \end{aligned}$$

Thus, the first term in the previous equation is the signal, and the second term is viewed as the noise in the worst case. We let $y_{2k} = j/\lambda$, $j \in \{0, 1, 2, 3, ..., \lambda\}$, $y_{2k} \in \{0/\lambda, 1/\lambda, 2/\lambda, ..., \lambda/\lambda\}$. The sufficient condition for recalling y_{1k} correctly is that the noise must be bounded as

$$\begin{aligned} y_{1k} - \frac{1}{2\lambda} &< y_{1k} \cdot 1^2 + (M-1) \cdot y_{2k} \cdot \left((u - 1/\lambda^2)/u\right)^{M^Z} \\ &< y_{1k} + \frac{1}{2\lambda} \quad (6) \end{aligned}$$

Here, we substitute $y_2k = j/\lambda$ into eqn. 6 and then simplify it as follows:

$$\left|(M-1) \cdot \left((u - 1/\lambda^2)/u\right)^{M^Z}\right| < \frac{1}{2j} \le \frac{1}{2} \quad (7)$$

The worst case will occur when $j = 1$, and we deem eqn. 7 to be the sufficient condition for the PBHC to accurately recall any desired pattern. Since the value of the polynomial in the absolute value of eqn. 7 is positive, the minimal Z in the worst case for the PBHC is derived in the following:

$$Z \ge (1/\ln M) \cdot \ln(\ln(1/2)/\ln((u - (1/\lambda^2))/u)) \quad (8)$$

where $u \le C_2^M \cdot (n + p) \le C_2^M \cdot (2n) \le M \cdot (M - 1) \cdot n$.

Eqn. 8 is the lower bound solution of Z, and according to eqn. 7, the minimal capacity can be derived as follows:

$$M \ge \left(\ln(1/2)/\ln((u - (1/\lambda^2))/u)\right)^{Z^{-1}}$$

where $u = M \cdot (M - 1) \cdot n$.

Results and conclusion: The BAM-like associative memory consists of two layers of neurons. One layer has n neurons and the other has p neurons. n is assumed to be less than or equal to p without any loss of robustness. In evaluating a BAM-like associative memory, probably the most important factor is its storage capacity. We consider that some randomly generated desired attractors can each be generally stored as a strong stable state in a BAM-like associative memory by the corresponding evolution equation [1].

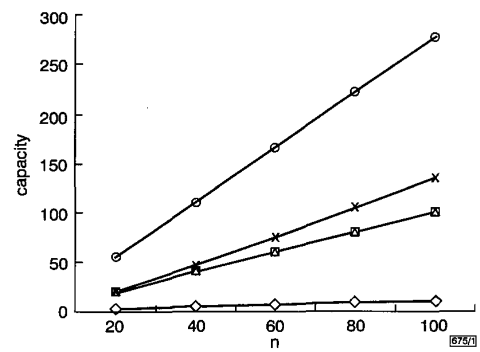

Fig. 1 *Capacity comparison of BAM-like hetero-associators*

—◇— Kosko BAM [1]
—□— SBAM [1]
—△— ABAM [1]
—×— GBAM [1]
—○— PBHC (λ = 2)

Table 1: Capacity comparison of Kosko BAM, SBAM, ABAM, GBAM and PBHC

Name \ n	20	40	60	80	100
Kosko BAM	3	5	7	9	10
SBAM	19	40	60	80	100
ABAM	20	40	60	80	100
GBAM	20	46	75	106	136
PBHC [λ = 2]	55	110	166	221	277

We find that the storage capacity of the GBAM is slightly higher than n, that of the SBAM or ABAM is closer or equal to n, and the capacity of the Kosko rule is $\le 0.15n$. By contrast, fuzzy data recognition using the PBHC provides a very high storage capacity for patterns. Table 1 and Fig. 1 present the capacity (M) for Kosko's BAM, SBAM, ABAM, GBAM and the PBHC with $\lambda = 2$, respectively. Significantly, we used the PBHC with $\lambda = 2$ in order to derive a fair comparison with other BAM-like designs which usually process either binary vectors or bipolar vectors. According to other simulation results, the capacity of the PBHC is $> 2n$ when $\lambda > 2$ and increases more than linearly as n increases. For instance, suppose $\lambda = 10$ ($Z = 3$), when n is equal to 30 and

60, we can obtain a capacity equal to 40006 and 84059, respectively. Therefore, the PBHC provides an extremely high storage capacity for pattern pairs. The practical capacity of the PBHC in the worst case is estimated, thereby allowing us to predetermine the size of the PBHC.

Acknowledgments: This research was partially supported by National Science Council under grant NSC 89-2219-E-110-001, 89-2215-E-110-014 and 89-2215-E-110-017.

5 August 1999
Electronics Letters Online No: 19991344
DOI: 10.1049/el:19991344

Chua-Chin Wang and Cheng-Fa Tsai (*Department of Electrical Engineering, National Sun Yat-Sen University, Kaohsiung, 80424 Taiwan, Republic of China*)

E-mail: ccwang@ee.nsysu.edu.tw

References

1 SHI, H., ZHAO, Y., and ZHAUNG, X.: 'A general model for bidirectional associative memories', *IEEE Trans. Syst. Man, Cybern. B: Cybern.*, 1998, **28**, (4), pp. 511–519
2 KOSKO, B.: 'Bidirectional associative memory', *IEEE Trans. Syst. Man, Cybern.*, 1988, **18**, (1), pp. 49–60
3 XU, Z.-B., LEUNG, Y., and HE, X.-W.: 'Asymmetric bidirectional associative memories', *IEEE Trans. Syst. Man, Cybern.*, 1994, **24**, pp. 1558–1564
4 CHUNG, F.-L., and LEE, T.: 'On fuzzy associative memory with multiple-rule storage capacity', *IEEE Trans. Fuzzy Syst.*, 1996, **4**, (3), pp. 375–384
5 ZHUANG, X., HUANG, Y., and CHEN, S.-S.: 'Better learning for bidirectional associative memory', *Neural Netw.*, 1993, **6**, (8), pp. 1131–1146

320 Gbit/s (8 × 40 Gbit/s) WDM transmission over 367 km with 120 km repeater spacing using carrier-suppressed return-to-zero format

Y. Miyamoto, A. Hirano, K. Yonenaga, A. Sano, H. Toba, K. Murata and O. Mitomi

The authors demonstrate +11 dBm-per-channel 320 Gbit/s (8 × 40 Gbit/s) WDM transmission over a 367 km zero-dispersion-flattened transmission line with 120 km repeater spacing using a nonlinearity-tolerant carrier-suppressed return-to-zero format.

Introduction: When targetting WDM systems with total capacities in excess of terabits per second, there are several advantages in increasing the electrical-time-division-multiplexed (ETDM) channel rate to 40 Gbit/s [1]. It is possible to reduce the number of multiplexed channels to less than 25, which simplifies network management and saves on wavelength resources. The channel power of such WDM systems should be linearly increased as the line rate increases in order to return the same signal-to-noise ratio. A numerical simulation has shown that the return-to-zero (RZ) format offers a large power margin in dispersion-managed transmission lines using singlemode fibre (SMF) at a line rate of 40 Gbit/s [2], and there are several experimental reports of using a dispersion-managed line [3 – 5]. No experimental report has, however, detailed 40 Gbit/s RZ channel WDM transmission performance at repeater-output powers > +10 dBm/channel, levels at which several fibre nonlinear effects, such as self-phase modulation (SPM) and cross-phase modulation (XPM), become significant in determining the system performance.

In this Letter, we show that our proposed optical-carrier-suppressed RZ (CS-RZ) format has a larger power margin than the conventional RZ signal format in an SMF-based, dispersion-managed transmission line (zero-dispersion-flattened (ZDF) transmission line [4]). We demonstrate 320 Gbit/s (8 × 40 Gbit/s) WDM transmission with 120 km repeater spacing for the first time over a 367 km ZDF transmission line. This is possible because the CS-RZ format achieves record 40 Gbit/s channel power of +11 dBm (total power: +20 dBm/8-channel).

Experimental setup: The experimental setup is shown in Fig. 1. In the transmitter, the eight optical carriers were simultaneously modulated with the 40 Gbit/s non-return-to-zero (NRZ) format ($2^7 - 1$ pseudorandom binary sequence) using an InP-HEMT multiplexer IC [6] and a push-pull type $LiNbO_3$ Mach-Zehnder (LN-MZ) modulator (MZ 1) [7]. The signal wavelengths ranged from 1546.1 nm (channel 1) to 1557.3 nm (channel 8) with 200 GHz spacing. The 40 Gbit/s NRZ optical signals were boosted and converted into 40 Gbit/s CS-RZ signals in a newly proposed MZ-modulator pulse generator. In the optical pulse generator, the LN-MZ modulator (MZ 2) [7] was biased at the transmission null.

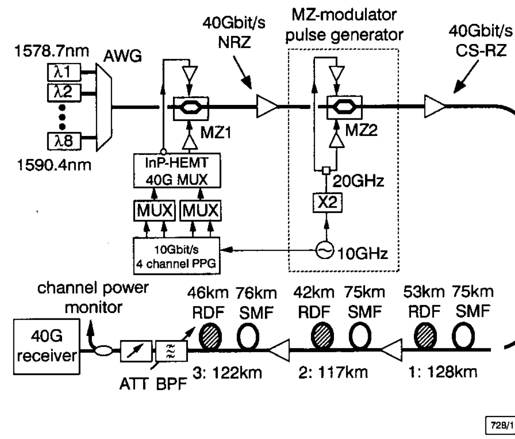

Fig. 1 *Experimental setup*

Two pairs of 20 GHz clock signals were fed to each electrode of the modulator (MZ 2). The phase-encoding characteristics of the modulator yielded a 40 GHz chirpless CS-RZ signal from a 20 GHz electrical input. The full width at half maximum (FWHM) measured by a streak camera was 12 ps. To generate a conventional RZ signal with an FWHM of 12 ps, the output of the MZ 2 modulator (driven by 40 GHz signals) was used with the normal bias condition: the mid-point between the transmission null and peak. The carrier component of the CS-RZ signal spectrum was suppressed and the spectral bandwidth of the CS-RZ signal was smaller than that of the conventional RZ signal, as shown in Fig. 2. In the receiver, the 320 Gbit/s signal was WDM-demultiplexed using a tunable bandpass filter with 0.9 nm bandwidth, and was optically demultiplexed into 20 Gbit/s signals to check the bit error rate (BER) [5]. The 367 km ZDF transmission line consisted of three repeater spans joined by two EDFA in-line repeaters. Each span consisted of SMF and reverse-dispersion fibre (RDF) [8]. The losses of the three sections were 29.06 dB (1: 0.23 dB/km), 28.04 dB (2: 0.24 dB/km) and 26.52 dB (3: 0.22 dB/km). The total dispersion of the 367 km ZDF line ranged from –3 ps/nm to +16 ps/nm over the 8-channel signal wavelengths, and a dispersion-flattened characteristic was obtained for a 10 nm wavelength range.

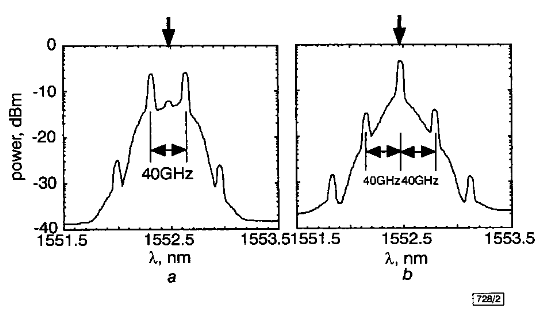

Fig. 2 *40 Gbit/s modulation spectra (↓: optical carrier frequency)*
a Proposed CS-RZ format
b Conventional RZ format

40 Gbit/s CS-RZ single-channel transmission: The CS-RZ and conventional RZ formats were compared in terms of single-channel transmission performance, both numerically simulated and meas-